

Cooper pairing and finite-size effects in a NJL-type four-fermion model

D. Ebert¹ and K. G. Klimenko²

¹ *Institute of Physics, Humboldt-University Berlin, 12489 Berlin, Germany*

² *IHEP and University "Dubna" (Protvino branch), 142281 Protvino, Moscow Region, Russia*

Starting from a NJL-type model with N fermion species fermion and difermion condensates and their associated phase structures are considered at nonzero chemical potential μ and zero temperature in spaces with nontrivial topology of the form $S^1 \otimes S^1 \otimes S^1$ and $R^2 \otimes S^1$. Special attention is devoted to the generation of the superconducting phase. In particular, for the cases of antiperiodic and periodic boundary conditions we have found that the critical curve of the phase transitions between the chiral symmetry breaking and superconducting phases as well as the corresponding condensates and particle densities strongly oscillate vs $\lambda \sim 1/L$, where L is the length of the circumference S^1 . Moreover, it is shown that at some finite values of L the superconducting phase transition is shifted to smaller values both of μ and particle density in comparison with the case of $L = \infty$.

PACS numbers: 11.30.Qc, 12.39.-x, 26.60.+c

Keywords: Nambu–Jona-Lasinio model; superconductivity; Dense fermion matter; finite-size effects

I. INTRODUCTION

Last years, great theoretical efforts are devoted to the understanding of the QCD phase diagram. Since at rather small values of baryonic density weak coupling perturbative QCD methods are not applicable, usually effective field theories such as the Nambu – Jona-Lasinio type models (NJL) [1] etc are invoked for such kind of investigations [2–7]. Evidently, at low temperatures and baryonic densities one deals with the hadronic phase. But at growing baryonic density, due to a condensation of Cooper pairs of two quarks (diquarks), there appears a phase transition to the so-called color superconducting (CSC) phase of QCD (see, e.g., the reviews [7]), where the color symmetry is spontaneously broken down. In particular, it turned out that NJL-type models are well-suited for the description of the chiral symmetry restoring phase transition and low-energy phenomenology of mesons [8] as well as of properties of CSC quark matter [7].

Since the most attractive feature of NJL models is the dynamical breaking of the chiral symmetry in the hadronic phase, the additional influence of different external factors on the chiral properties of these models was also studied extensively. For example, they were used to investigate dense baryonic matter in the presence of external (chromo)magnetic fields [9]. In particular, it was demonstrated on the basis of NJL models in diverse dimensions that both external magnetic [10] and chromomagnetic [11] fields induce the chiral symmetry breaking. Moreover, chiral symmetry breaking in four-fermion models was studied in weakly curved spaces [12, 13] and in spaces with nontrivial topology, when one or more space coordinates were compactified [14–16]. In addition, the properties of finite size normal quark matter droplets in the language of the MIT-bag model were investigated, e.g., in the review [17]. Recently, it was also noted that the position of the chiral critical end point of the QCD phase diagram, which could be investigated in heavy ion collision experiments, depends essentially on the finite system sizes [18].

There is also some progress in the understanding of the influence of different external factors on the CSC phase transition. In this context it is worth mentioning that an external chromomagnetic field induces the CSC phase transition [19] and that an external magnetic field leads to the appearance of new magnetic phases in the three-flavor color superconducting quark matter [20]. Moreover, the effect of spaces with constant curvature on CSC was studied in [21]. Note also that the stability of finite size quark matter droplets in the color-flavor locked phase was investigated in the framework of a bag model using the so-called multiple expansion method [22].

In the present work we shall use an alternative approach in order to investigate superconductivity in dense cold fermionic matter placed in a finite volume. In particular, we shall study the Cooper pairing phenomenon in the framework of a NJL model describing the interaction of N fermion species in compactified spaces with nontrivial topology. As in QCD, this model ensures in the usual R^3 -space the chiral symmetry breaking at rather small values of the chemical potential μ , whereas at large values of μ there appears a superconducting phase due to the condensation of difermions.

In this context, let us recall the well-known fact that spontaneous symmetry breaking in low dimensional quantum field theories may become impossible due to strong quantum fluctuations of fields [23]. The same is also true for systems that occupy a limited space volume. However, as it is clear from physical considerations, the finite size in itself may in some situations not forbid the spontaneous symmetry breaking, if the characteristic length of the region of space occupied by the system is much greater than the Compton wavelength of the excitations responsible for tunneling and restoration of symmetry. (Indeed, one may recall here well known physical phenomena such as the superfluidity of Helium or superconductivity of metals that are observed in samples of finite volume). This idea has been discussed for some scalar field theories as well as for NJL models in a closed Einstein universe, for instance, in [24]. Similarly, if quantum fluctuations of fields are suppressed when the number of quantum fields N tends to infinity,

spontaneous symmetry breaking might even occur in a finite volume. Indeed, suppose that in a finite volume an effective potential of an $O(N)$ -symmetrical model has degenerate global minima. Then, in D -dimensional spacetime the transition probability from one minimum to another is proportional to $\exp(-NL^{D-2})$ at zero temperature, where L is the linear size of the system [25]. It follows from this expression that if L and N are finite, the transition probability is nonzero. This circumstance ensures the vanishing of the order parameter and, as a result, might lead to a prohibition for spontaneous symmetry breaking in a finite volume. However, if $N \rightarrow \infty$ the transition probability vanishes and the spontaneous symmetry breaking is allowed.

In the present paper, the consideration of Cooper pair (difermion) condensation in restricted regions of space is performed in a toy NJL model in the mean field approximation, i.e. in the leading order of the large N -expansion technique at $T = 0$. In particular, in order to be sure that the obtained results are stable against quantum fluctuations, the composite difermion field must be a flavor singlet (like the composite fermion-antifermion field) which technically leads to an N -factor in the part of the effective action arising from fermion loops and thus guarantees the application of the $1/N$ expansion. It is just by this reason that we demand here $O(N)$ flavor symmetry as opposed to the usual $SU(N)$ symmetry.¹

The paper is organized as follows. For comparison, we first derive in Section II the expression for the thermodynamic potential of cold dense fermionic matter, described by a NJL-type Lagrangian, for the case of R^3 space. It is shown here that for some fixed values of coupling constants two phases are allowed, the chiral symmetry breaking phase (at $\mu < \mu_c \approx 0.3$ GeV) and the superconducting one (at $\mu > \mu_c$). In Section III the phase structure of the model is investigated in the $S^1 \otimes S^1 \otimes S^1$ space with periodic and antiperiodic boundary conditions for fermion fields. We have found a rather rich phase structure in the $(\mu, \lambda \sim 1/L)$ -plane, where L is the length of each circumference S^1 . It turns out that the boundary between the chiral symmetry breaking and superconducting phases as well as the corresponding condensate values and particle densities strongly oscillate vs λ at $\lambda \rightarrow 0$. Finally, in Section IV similar considerations were performed in the case of $R^2 \otimes S^1$ space topology, where we have found smoother oscillations of both the critical curve and the condensates vs λ .

II. THE CASE OF R^3 SPACE

A. The model and its thermodynamic potential

Our investigation is based on an NJL-type model with massless fermions belonging to a fundamental multiplet of the $O(N)$ flavor group. Its Lagrangian describes the interaction in the fermion-antifermion as well as scalar difermion channels:

$$L = \sum_{k=1}^N \bar{\psi}_k \left[\gamma^\nu i \partial_\nu + \mu \gamma^0 \right] \psi_k + \frac{G}{N} \left(\sum_{k=1}^N \bar{\psi}_k \psi_k \right)^2 + \frac{H}{N} \left(\sum_{k=1}^N \bar{\psi}_k^C i \gamma^5 \psi_k \right) \left(\sum_{j=1}^N \bar{\psi}_j i \gamma^5 \psi_j^C \right), \quad (1)$$

where μ is a fermion number chemical potential. As it is noted above, all fermion fields ψ_k ($k = 1, \dots, N$) form a fundamental multiplet of $O(N)$ group. Moreover, each field ψ_k is a four-component Dirac spinor; $\psi_k^C = C \bar{\psi}_k^t$ and $\bar{\psi}_k^C = \psi_k^t C$ are charge-conjugated spinors, and $C = i \gamma^2 \gamma^0$ is the charge conjugation matrix (the symbol t denotes the transposition operation). Clearly, the Lagrangian L is invariant under transformations from the internal $O(N)$ group, which is introduced here in order to make it possible to perform all the calculations in the framework of the nonperturbative large- N expansion method. Physically more interesting is that the model (1) is invariant under transformations from an Abelian electric charge $U(1)$ group: $\psi_k \rightarrow \exp i \alpha \psi_k$ ($k = 1, \dots, N$). In addition, the Lagrangian is invariant under the discrete γ^5 chiral transformation: $\psi_k \rightarrow \gamma^5 \psi_k$, $\bar{\psi}_k \rightarrow -\bar{\psi}_k \gamma^5$ ($k = 1, \dots, N$). The linearized version of Lagrangian (1) that contains auxiliary scalar bosonic fields $\sigma(x)$, $\Delta(x)$, $\Delta^*(x)$ has the following form

$$\mathcal{L} = \bar{\psi}_k \left[\gamma^\nu i \partial_\nu + \mu \gamma^0 - \sigma \right] \psi_k - \frac{N}{4G} \sigma^2 - \frac{N}{4H} \Delta^* \Delta - \frac{\Delta^*}{2} [\bar{\psi}_k^C i \gamma^5 \psi_k] - \frac{\Delta}{2} [\bar{\psi}_k i \gamma^5 \psi_k^C]. \quad (2)$$

(Here and in the following summation over repeated indices $k = 1, \dots, N$ is implied.) Clearly, the Lagrangians (1) and (2) are equivalent, as can be seen by using the Euler-Lagrange equations of motion for scalar bosonic fields $\sigma(x)$, $\Delta(x)$, $\Delta^*(x)$, which take the form

$$\sigma(x) = -2 \frac{G}{N} (\bar{\psi}_k \psi_k), \quad \Delta(x) = -2 \frac{H}{N} (\bar{\psi}_k^C i \gamma^5 \psi_k), \quad \Delta^*(x) = -2 \frac{H}{N} (\bar{\psi}_k i \gamma^5 \psi_k^C). \quad (3)$$

¹ Note the important difference to the case of QCD-like NJL models with $SU(N)$ color symmetry, where the usual $1/N$ expansion cannot be applied to *colored diquarks* due to the lack of a corresponding N factor from quark loops.

One can easily see from (3) that the (neutral) field $\sigma(x)$ is a real quantity, i.e. $(\sigma(x))^\dagger = \sigma(x)$ (the superscript symbol \dagger denotes the hermitian conjugation), but the (charged) difermion field $\Delta(x)$ is a complex scalar, so $(\Delta(x))^\dagger = \Delta^*(x)$. Clearly, all the fields (3) are singlets with respect to the $O(N)$ group.² If the scalar difermion field $\Delta(x)$ has a nonzero ground state expectation value, i.e. $\langle \Delta(x) \rangle \neq 0$, the Abelian $U(1)$ charge symmetry of the model is spontaneously broken down. However, if $\langle \sigma(x) \rangle \neq 0$ then the discrete chiral symmetry of the model is spontaneously broken.

Let us now study the phase structure of the four-fermion model (1) by starting with the equivalent semi-bosonized Lagrangian (2). In the leading order of the large- N approximation, the effective action $\mathcal{S}_{\text{eff}}(\sigma, \Delta, \Delta^*)$ of the considered model is expressed by means of the path integral over fermion fields:

$$\exp(i\mathcal{S}_{\text{eff}}(\sigma, \Delta, \Delta^*)) = \int \prod_{l=1}^N [d\bar{\psi}_l][d\psi_l] \exp\left(i \int \mathcal{L} d^4x\right),$$

where

$$\mathcal{S}_{\text{eff}}(\sigma, \Delta, \Delta^*) = - \int d^4x \left[\frac{N}{4G} \sigma^2(x) + \frac{N}{4H} \Delta(x) \Delta^*(x) \right] + \tilde{\mathcal{S}}_{\text{eff}}. \quad (4)$$

The fermion contribution to the effective action, i.e. the term $\tilde{\mathcal{S}}_{\text{eff}}$ in (4), is given by:

$$\exp(i\tilde{\mathcal{S}}_{\text{eff}}) = \int \prod_{l=1}^N [d\bar{\psi}_l][d\psi_l] \exp\left(\frac{i}{2} \int [\bar{\psi}_k D^+ \psi_k + \bar{\psi}_k^C D^- \psi_k^C - \bar{\psi}_k K \psi_k^C - \bar{\psi}_k^C K^* \psi_k] d^4x\right), \quad (5)$$

where we have used the following notations³

$$D^\pm = i\gamma^\nu \partial_\nu \pm \mu\gamma^0 - \sigma(x), \quad K^* = i\Delta^*(x)\gamma^5, \quad K = i\Delta(x)\gamma^5. \quad (6)$$

In the following, it is very convenient to use the Nambu–Gorkov formalism, in which for each fixed $k = 1, \dots, N$ a pair of fermion fields ψ_k and ψ_k^C are composed into a bispinor Ψ_k such that

$$\Psi_k = \begin{pmatrix} \psi_k \\ \psi_k^C \end{pmatrix}, \quad \Psi_k^t = (\psi_k^t, \bar{\psi}_k^C{}^t); \quad \bar{\Psi}_k = (\bar{\psi}_k, \bar{\psi}_k^C) = (\bar{\psi}_k, \psi_k^t C) = \Psi_k^t \begin{pmatrix} 0 & C \\ C & 0 \end{pmatrix} \equiv \Psi_k^t Y. \quad (7)$$

Furthermore, by introducing the matrix-valued operator

$$Z = \begin{pmatrix} D^+ & -K \\ -K^* & D^- \end{pmatrix}, \quad (8)$$

one can rewrite the gaussian functional integral in (5) in terms of Ψ_k and Z and then evaluate it as follows (clearly, in this case $[d\bar{\psi}_k][d\psi_k] = [d\bar{\psi}_k^C][d\psi_k^C] = [d\Psi_k]$):

$$\exp(i\tilde{\mathcal{S}}_{\text{eff}}) = \int \prod_{l=1}^N [d\Psi_l] \exp\left\{\frac{i}{2} \int \bar{\Psi}_k Z \Psi_k d^4x\right\} = \int \prod_{l=1}^N [d\Psi_l] \exp\left\{\frac{i}{2} \int \Psi_k^t (YZ) \Psi_k d^4x\right\} = \det^{N/2}(YZ) = \det^{N/2}(Z),$$

where the last equality is valid due to the evident relation $\det Y = 1$. Then, using the relation (4), one obtains the expression for the effective action:

$$\mathcal{S}_{\text{eff}}(\sigma, \Delta, \Delta^*) = - \int d^4x \left[\frac{N}{4G} \sigma^2(x) + \frac{N}{4H} \Delta(x) \Delta^*(x) \right] - i \frac{N}{2} \ln \det(Z) \quad (9)$$

Starting from (9), one can define the thermodynamic potential (TDP) $\Omega(\sigma, \Delta, \Delta^*)$ of the model (1) in the leading order of the large- N expansion (mean field approximation):

$$\mathcal{S}_{\text{eff}} \Big|_{\sigma, \Delta, \Delta^* = \text{const}} = -N\Omega(\sigma, \Delta, \Delta^*) \int d^4x. \quad (10)$$

Here we have supposed that the quantities σ, Δ, Δ^* do not depend on coordinates x . Moreover, without loss of generality, one can set the arbitrary phase of Δ equal to zero so that Δ is now considered as a non-negative real

² Note that the $\Delta(x)$ field is a flavor $O(N)$ singlet, since the representations of this group are real.

³ In order to bring the fermion sector of the Lagrangian (2) to the expression, given in the square brackets of (5), we use the following well-known relations: $\partial_\nu^t = -\partial_\nu$, $C\gamma^\nu C^{-1} = -(\gamma^\nu)^t$, $C\gamma^5 C^{-1} = (\gamma^5)^t = \gamma^5$.

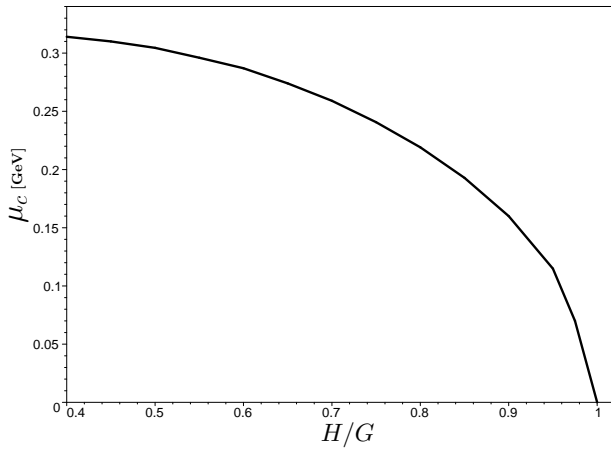


FIG. 1: The case of R^3 space topology: The behavior of the critical value of the chemical potential μ_c vs H at $G = 30.06 \text{ GeV}^{-2}$.

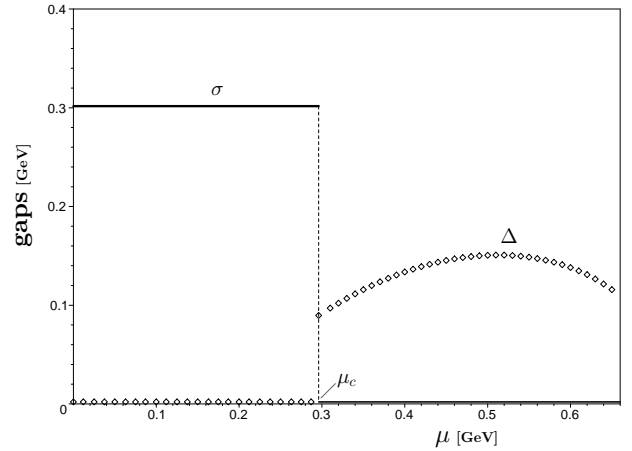


FIG. 2: The case of R^3 space topology: The gaps σ and Δ vs μ , where $\mu_c \approx 296 \text{ MeV}$.

quantity, i.e. $\Delta = |\Delta|$. As a consequence, the $\det Z$ in (9) and the TDP (10) are easily calculated. Indeed, using the general formulae

$$\det \begin{pmatrix} A & B \\ \bar{A} & \bar{B} \end{pmatrix} = \det[-\bar{A}B + \bar{A}A\bar{A}^{-1}\bar{B}]$$

and $\det O = \exp \text{Tr} \ln O$, one can find for the TDP (10) the expression:

$$\Omega(\sigma, \Delta) = \frac{\sigma^2}{4G} + \frac{\Delta^2}{4H} + \frac{i}{2} \frac{\text{Tr}_{sx} \ln D}{\int d^4x}, \quad (11)$$

where $D = \Delta^2 + \gamma^5 D^+ \gamma^5 D^-$ and the Tr -operation stands for the trace in spinor (s) and four-dimensional coordinate (x) spaces, respectively. Transferring in (11) to the momentum space representation for the operator D , we have

$$\Omega(\sigma, \Delta) = \frac{\sigma^2}{4G} + \frac{\Delta^2}{4H} + \frac{i}{2} \text{Tr}_s \int \frac{d^4p}{(2\pi)^4} \ln \left[\Delta^2 + \gamma^5 (\not{p} + \mu \gamma^0 - \sigma) \gamma^5 (\not{p} - \mu \gamma^0 - \sigma) \right], \quad (12)$$

where in the square brackets just the momentum space representation, \bar{D} , for the operator D appears. In four-dimensional spinor space the 4×4 matrix \bar{D} has two different eigenvalues ϵ_{\pm} , each being two-fold degenerate:

$$\epsilon_{\pm} = (E_{\Delta}^{\pm})^2 - p_0^2 \equiv (E \pm \mu)^2 + \Delta^2 - p_0^2, \quad (13)$$

where $E = \sqrt{\sigma^2 + \vec{p}^2}$. Since $\text{Tr}_s \ln \bar{D} = 2 \ln \epsilon_+ \epsilon_-$, one can integrate in (12) over p_0 and obtain the following expression for the TDP of dense cold fermion matter (more details of this technique are presented, e.g., in [26]):

$$\Omega(\sigma, \Delta) = \frac{\sigma^2}{4G} + \frac{\Delta^2}{4H} - \int \frac{d^3p}{(2\pi)^3} \Theta(\Lambda^2 - \vec{p}^2) [E_{\Delta}^+ + E_{\Delta}^-], \quad (14)$$

where the Heaviside step-function $\Theta(x)$ has been inserted in order to regularize the ultraviolet divergent integral, and Λ is a cutoff parameter that is usually taken smaller than 1 GeV, i.e. $\Lambda < 1 \text{ GeV}$. Since the TDP (14) is symmetric with respect to the transformations $\sigma \rightarrow -\sigma$, and $\mu \rightarrow -\mu$, we suppose in the following that $\sigma \geq 0$ and $\mu \geq 0$ (recall also $\Delta \geq 0$). It is important to note that the quantities E_{Δ}^- and E_{Δ}^+ defined in (13) are the energies of fermions and antifermions (quasiparticles) in a medium, correspondingly. Clearly, each energy level is infinitely degenerated with respect to the direction of the momentum \vec{p} . Indeed, there are infinitely many quasiparticles with the same energy but with different directions of momenta.

B. Phase structure

In order to obtain the phase structure of the initial model it is necessary to investigate the behavior of the global minimum point (GMP) of the TDP (14) in dependence on the chemical potential μ . The coordinates of this point are usually called gaps. (The σ - and Δ -coordinates of the GMP are the chiral and difermion condensates, respectively.) In

the model two types of the GMPs are allowed, i) $(\sigma \neq 0, 0)$ and ii) $(0, \Delta \neq 0)$. The GMP of the i)-th type corresponds to the phase with broken chiral γ^5 -invariance only (it is a so-called normal phase), whereas the GMP of the type ii) corresponds to the superconducting phase, in which Cooper pairing of fermions leads to the spontaneous breaking of the $U(1)$ symmetry.

Throughout the paper, we use in our numerical calculations the value $G = 30.06 \text{ GeV}^{-2}$. Moreover, for illustrations, let us take the cutoff in the momentum integral in (14) to be $\Lambda = 650 \text{ MeV}$. For this choice of parameters, the TDP (14) then predicts at $\mu = 0$ and $H = 0$ (the last is equivalent to the constraint $\Delta = 0$) a corresponding value of the chiral condensate which is characteristic to some low energy phenomenological QCD-like NJL models [7]. In the case under consideration the phase structure of the model depends essentially on the value of the coupling constant H . Numerical calculations show that at $H < G$ and sufficiently low values of $\mu < \mu_c$ the GMP of the TDP (14) corresponds to the normal phase of the model. However, at $\mu > \mu_c$ the superconducting phase is realized. If $H > G$, then for all values of μ , and even for $\mu = 0$, the ground state of the system corresponds to the superconducting phase. The behavior of the critical value of the chemical potential μ_c vs H is depicted in Fig. 1. (At the same time, one may consider Fig. 1 as a phase portrait of the model in terms of μ and H . Then, below (above) the critical line μ_c the normal (superconducting) phase of the model is realized.) In all subsequent numerical calculations the coupling constant H is fixed by the relation $H = 0.55 G$. Hence, the set of model parameters in our investigations is the following:

$$G = 30.06 \text{ GeV}^{-2}, \quad H = 0.55 G, \quad \Lambda = 650 \text{ MeV}. \quad (15)$$

As a result, we have for the set (15) $\mu_c \approx 0.3 \text{ GeV}$. Moreover, the behavior of gaps σ and Δ vs μ in this case is presented in Fig. 2. It is clear from this figure that at $\mu < \mu_c$ the GMP of the TDP (14) has the form $(\sigma, 0)$ (as a consequence, the system is in the normal phase), where $\sigma \approx 0.3 \text{ GeV}$, whereas for $\mu > \mu_c$ the superconducting phase, corresponding to the GMP of the form $(0, \Delta)$ of the TDP, is realized in the system. Evidently, in the critical point μ_c there is a first order phase transition.

III. THE CASE OF $S^1 \otimes S^1 \otimes S^1$ SPACE TOPOLOGY

In the present section we generalize the previously obtained results to the case of a space with finite volume. Evidently, this is a reasonable task, since all physical effects take place in restricted space regions. For simplicity, let us suppose that our system is immersed into a box with equal linear sizes, $0 \leq x, y, z \leq L$. It is well known that in this case the task is equivalent to the consideration of the model in the space of nontrivial $S^1 \otimes S^1 \otimes S^1$ topology with quantum fields satisfying some boundary conditions of the form (here we again simplify the problem, demanding identical boundary conditions for all coordinates):

$$\psi_k(t, x + L, y, z) = e^{i\pi\alpha} \psi_k(t, x, y, z), \quad \psi_k(t, x, y + L, z) = e^{i\pi\alpha} \psi_k(t, x, y, z), \quad \psi_k(t, x, y, z + L) = e^{i\pi\alpha} \psi_k(t, x, y, z) \quad (16)$$

where $0 \leq \alpha < 2$, L is the length of the circumference S^1 , and now each of the variables x, y, z mean the path along it. Below, we shall use only two values of the parameter α : $\alpha = 0$ for periodic boundary conditions and $\alpha = 1$ for the antiperiodic one.

As a consequence, to obtain the thermodynamic potential $\Omega_{L\alpha}(\sigma, \Delta)$ of fermions moving in a space with nontrivial topology $S^1 \otimes S^1 \otimes S^1$, we should replace the integration over each momentum in (14) by a summation over corresponding discrete momenta $p_{n\alpha}$ following the rule:

$$\int \frac{d^3p}{(2\pi)^3} f(p_x, p_y, p_z) \rightarrow \frac{1}{L^3} \sum_{k=-\infty}^{\infty} \sum_{l=-\infty}^{\infty} \sum_{m=-\infty}^{\infty} f(p_{k\alpha}, p_{l\alpha}, p_{m\alpha}), \quad p_{n\alpha} = \frac{\pi}{L}(2n + \alpha), \quad n = 0, \pm 1, \pm 2, \dots \quad (17)$$

A. The case of antiperiodic boundary conditions

Applying the rule (17) with $\alpha = 1$ in the expression (14), one immediately obtains the TDP of the system in the case of antiperiodic (“a”) boundary conditions:

$$\Omega_{La}(\sigma, \Delta) = \frac{\sigma^2}{4G} + \frac{\Delta^2}{4H} - \frac{8\lambda^3}{\pi^3} \sum_{i=0}^{\infty} \sum_{k=0}^{\infty} \sum_{l=0}^{\infty} \Theta(\Lambda^2 - p_{ia}^2 - p_{ka}^2 - p_{la}^2) \left[\mathcal{E}_{\Delta ikl}^+ + \mathcal{E}_{\Delta ikl}^- \right], \quad (18)$$

where $\lambda = \pi/L$, $\mathcal{E}_{\Delta ikl}^{\pm} = \sqrt{(\mathcal{E}_{ikl} \pm \mu)^2 + \Delta^2}$, $\mathcal{E}_{ikl} = \sqrt{p_{ia}^2 + p_{ka}^2 + p_{la}^2 + \sigma^2}$, and $p_{ia} = \lambda(2i + 1)$ etc.

The quantities $\mathcal{E}_{\Delta ikl}^{\pm}$ in (18) are the energies of elementary one-fermion excitations (quasiparticles) in a dense medium which occupies now a finite volume and is constrained by antiperiodic boundary conditions. (The signs $-/+$ correspond to the energies of fermion/antifermion quasiparticles.) Evidently, both fermion and antifermion quasiparticle energy

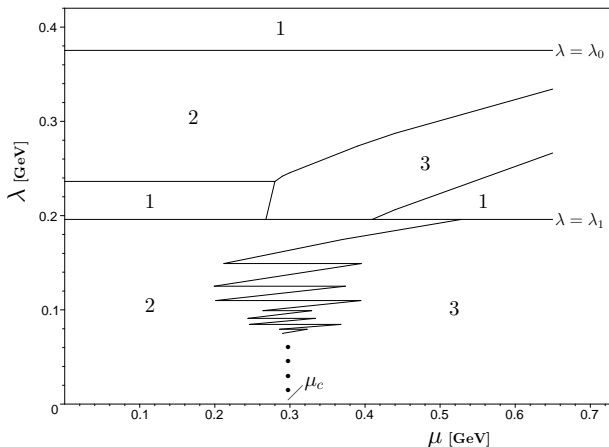


FIG. 3: Phase structure in the case of $S^1 \otimes S^1 \otimes S^1$ space topology with antiperiodic boundary conditions. The numbers 1, 2 and 3 denote the symmetric phase with $\sigma = 0, \Delta = 0$, the chirally broken phase with $\sigma \neq 0, \Delta = 0$ and the superconducting phase with $\sigma = 0, \Delta \neq 0$, correspondingly. Here $\lambda = \pi/L$, $\mu_c \approx 0.296$ GeV, $\lambda_0 \approx 0.375$ GeV, $\lambda_1 \approx 0.195$ GeV.

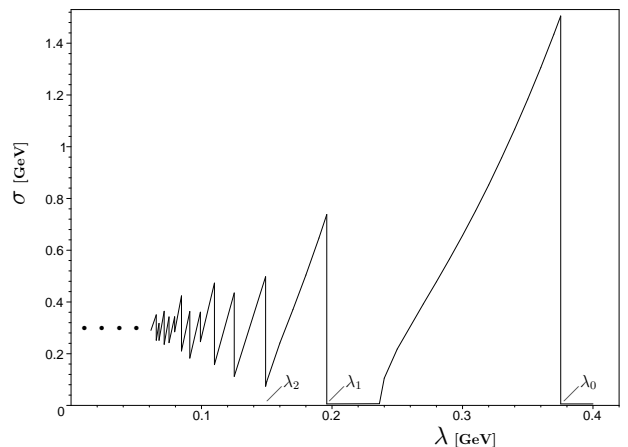


FIG. 4: The gap σ vs $\lambda = \pi/L$ at $\mu = 0.18$ GeV in the case of $S^1 \otimes S^1 \otimes S^1$ space topology with antiperiodic boundary conditions. Here $\lambda_0 \approx 0.375$ GeV, $\lambda_1 \approx 0.195$ GeV, $\lambda_2 \approx 0.149$ GeV.

levels can be labeled by a triple of integers, (i, k, l) , where $i \geq k \geq l \geq 0$. Clearly, in a finite volume the degeneracy of quasiparticle energy levels are partially (or even totally) removed. For example, each energy level with quantum numbers $(0, 0, 0)$ is non-degenerated, the level $(1, 0, 0)$ is three-fold degenerated etc. Now, for each energy level (i, k, l) let us put into correspondence the integer $N_{ikl} = (2i + 1)^2 + (2k + 1)^2 + (2l + 1)^2$ and, as a result, the real quantity $\lambda_{ikl} \equiv \sqrt{\Lambda^2/N_{ikl}}$.⁴ Using these definitions, we construct an infinite set of real scales of the form

$$\lambda_0 > \lambda_1 > \lambda_2 > \dots > \lambda_n > \dots, \quad (19)$$

where each scale λ_k coincides with one of the above obtained expressions λ_{ikl} and vice versa, each quantity λ_{ikl} is equal to some element of the sequence (19). So, $\lambda_0 = \sqrt{\Lambda^2/3} = \lambda_{000} \approx 0.375$ GeV, $\lambda_1 = \sqrt{\Lambda^2/11} = \lambda_{100} \approx 0.195$ GeV, $\lambda_2 = \sqrt{\Lambda^2/19} = \lambda_{110} \approx 0.149$ GeV, $\lambda_3 = \sqrt{\Lambda^2/27} = \lambda_{111} = \lambda_{200} \approx 0.125$ GeV, $\lambda_4 = \sqrt{\Lambda^2/35}$ etc.

Recall that our aim is to investigate the phase structure of the system with the TDP presented in (18). This means that it is necessary to study the behavior of the global minimum point (GMP) of the TDP vs μ and λ (or L). The structure of the TDP (18) suggests the following strategy for studying the corresponding GMP. Let us divide the plane (μ, λ) into an infinite set of strips, parallel to the μ -axis:

$$\omega_0 = \{(\mu, \lambda) : \lambda > \lambda_0\}, \omega_1 = \{(\mu, \lambda) : \lambda_0 > \lambda > \lambda_1\}, \dots, \omega_n = \{(\mu, \lambda) : \lambda_{n-1} > \lambda > \lambda_n\}, \dots \quad (20)$$

Due to the presence of the theta-function in (18), each sum is indeed a finite one there. Furthermore, for the values of (μ, λ) from the strip ω_0 the argument of the theta-function is negative and hence the term with sums vanishes there. We see that in this case the TDP is reduced to the quantity $\Omega_{La0} = (\sigma^2/4G + \Delta^2/4H)$ whose minimum lies at the point $(\sigma = 0, \Delta = 0)$. As a result, all the points of the strip ω_0 correspond to the symmetric phase of the model (see Fig. 3). If the point (μ, λ) belongs to the strip ω_1 , then only the energy levels with quantum numbers $(0, 0, 0)$ contribute to the sum in (18), so the TDP (18) reduces to the quantity Ω_{La1} ,

$$\Omega_{La1} = \frac{\sigma^2}{4G} + \frac{\Delta^2}{4H} - \frac{8\lambda^3}{\pi^3} \left[\sqrt{\left(\sqrt{\sigma^2 + 3\lambda^2 + \mu}\right)^2 + \Delta^2} + \sqrt{\left(\sqrt{\sigma^2 + 3\lambda^2 - \mu}\right)^2 + \Delta^2} \right]. \quad (21)$$

The form of the GMP of this function depends essentially on the values of (μ, λ) , so in the strip ω_1 , as numerical calculations show, there are three different phases (see Fig. 3): the symmetric phase 1 corresponding to the GMP of the form $(\sigma = 0, \Delta = 0)$, the chirally broken phase 2 with $(\sigma \neq 0, \Delta = 0)$ and superconducting (SC) phase 3 with $(\sigma = 0, \Delta \neq 0)$.

⁴ It might occur that for energy levels with different quantum numbers (i, k, l) there arises the same integer N_{ikl} . For example, for the energy levels with quantum numbers $(1, 1, 1)$ and $(2, 0, 0)$ we have $N_{111} = N_{200} = 27$ etc.

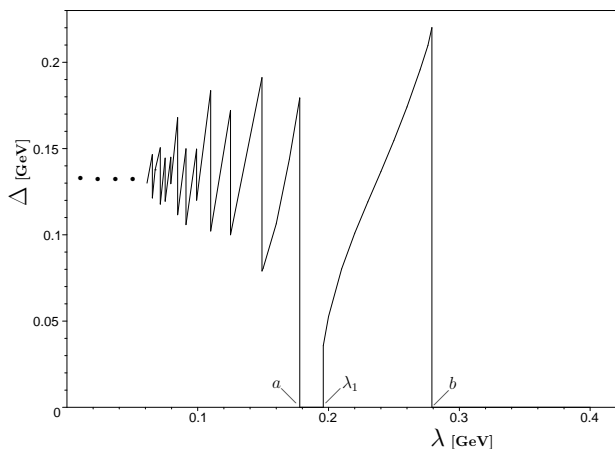


FIG. 5: The gap Δ vs λ at $\mu = 0.4$ GeV in the case of $S^1 \otimes S^1 \otimes S^1$ space topology with antiperiodic boundary conditions. Here $a \approx 0.178$ GeV, $b \approx 0.279$ GeV and other notations are presented in Figs 3, 4.

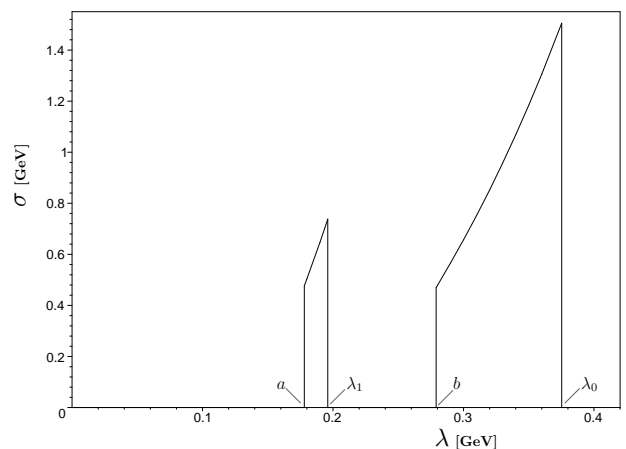


FIG. 6: The gap σ vs λ at $\mu = 0.4$ GeV in the case of $S^1 \otimes S^1 \otimes S^1$ space topology with antiperiodic boundary conditions. The notations are the same as in Figs 3-5.

To study the phase structure of the model in the strip ω_2 , it is necessary to take into account in the sums (18) the contribution from the energy levels $(1, 0, 0)$ in addition. In the strip ω_3 the energy levels with quantum numbers $(1, 1, 0)$ should be switched on in addition to the previous ones, and so on. However, in each of the strips ω_k with $k \geq 2$ only the phases 2 and 3 might exist, so for all $\lambda < \lambda_1$ we have found in the plane (μ, λ) just these two phases, the phase with broken chiral symmetry and the superconducting one. In Fig. 3 they are arranged below the line $\lambda = \lambda_1$ and divided by a zigzag, or oscillating, critical line. The amplitude of oscillations of this line is rather large for values of λ near the value λ_1 . However, when λ decreases, the amplitude of oscillations becomes smaller and smaller, and this critical line, or the boundary between phases 2 and 3, tends as a whole to the point $(\mu_c, 0)$ at $\lambda \rightarrow 0$, where μ_c is the critical chemical potential at $L = \infty$. Moreover, it is clear from Fig. 3 that at some values of λ the SC phase is allowed at even smaller values of μ (up to values $\mu \approx 0.2$ GeV) than it occurs at $L = \infty$.

In Fig. 4 the behavior of the gap σ vs λ at $\mu = 0.18$ GeV is depicted (at this value of μ the gap Δ equals to zero). In Figs 5, 6 the gaps Δ and σ vs λ are represented at $\mu = 0.4$ GeV, correspondingly. As it is clear from Figs 3-5, the oscillations both of the critical line and gaps are characteristic features of the model in the finite volume. Clearly, these quantities oscillate strongly vs λ . One should also take into account that the gaps σ and Δ from Figs 4-6 are really discontinuous functions vs λ in the points $\lambda_0, \lambda_1, \lambda_2$ etc.

Finally, let us discuss the influence of a nontrivial topology on the values of particle density $n_\mu(\lambda) = -\partial\Omega_{La}/\partial\mu$ in the SC phase. In Fig. 7 its behavior vs λ is presented at fixed $\mu = 0.4$ GeV in comparison with the particle density at $\lambda = 0$ ($L = \infty$). It is clear from this figure that at some finite values of L which correspond to values of λ from rather small vicinities of λ_k ($k = 2, 3, \dots$) the superconducting phase is realized at smaller particle densities than at $L = \infty$ (in these cases the ratio $n_\mu(\lambda)/n_\mu(0)$ is less than 1) and at the same value of $\mu = 0.4$ GeV. It was mentioned above that the SC phase may occur even at $\mu < \mu_c$ if L is finite (see Fig. 3). It is interesting to note that in these cases the particle density can also reach rather small values. For example, it turns out that the point $(\mu = 0.21, \lambda = 0.1255)$ GeV lies in the SC phase (see Fig. 3). Numerical calculations show that for this set of parameters the density of particles $n_\mu(\lambda)$ inside SC matter is much smaller than n_c , where n_c is the density at $\mu = \mu_c$ and $L = \infty$, since in this case we have $n_\mu(\lambda) \approx 0.36 n_c$. These facts might be understood by taking into account the results of the papers [17, 22], where in particular it was shown that the actual baryonic chemical potential, i.e. the energy per one baryon, increases with decreasing size L of a system. Hence, for rather small values of the chemical potential μ , for example at $\mu < \mu_c$, by decreasing L , it is in principle possible, to reach the value of the actual baryonic chemical potential at which the SC gap Δ is opened, although in R^3 -space the superconducting phase is not realized at the same value of $\mu < \mu_c$.

Note that the above mentioned as well as the following results should be taken with caution when $\lambda \gtrsim \Lambda$. The reason is that in this case the infrared cutoff λ comes closer to the ultraviolet one Λ , and thus the phase space is decreased due to the presence of the θ -function, e.g., in the expression (18).

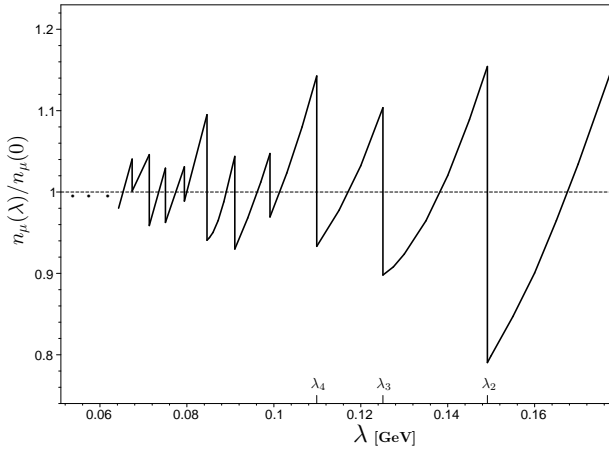


FIG. 7: Ratio of particle densities $\frac{n_\mu(\lambda)}{n_\mu(0)}$ vs λ at $\mu = 0.4$ GeV in the case of $S^1 \otimes S^1 \otimes S^1$ space topology with antiperiodic boundary conditions. (The quantities λ_k are presented in the text below eq.(19).)

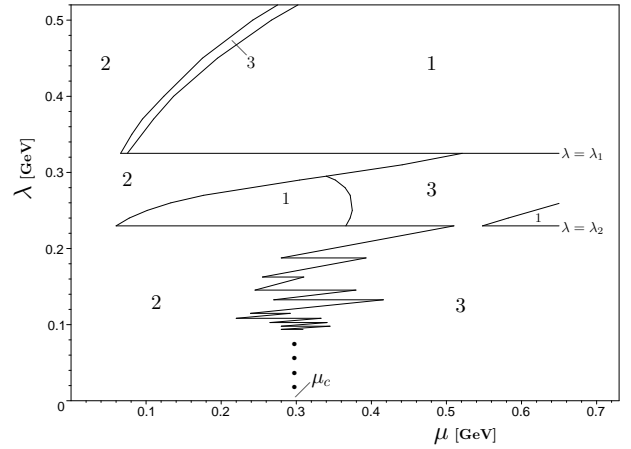


FIG. 8: Phase structure in the case of $S^1 \otimes S^1 \otimes S^1$ space topology with periodic boundary conditions. Here $\lambda_1 = 0.325$ GeV, $\lambda_2 \approx 0.223$ GeV and other notations are given in Fig. 3.

B. The case of periodic boundary conditions

Applying the rule (17) with $\alpha = 0$ in the expression (14), we immediately obtain the TDP of the system in the case of periodic (“p”) boundary conditions:

$$\Omega_{Lp}(\sigma, \Delta) = \frac{\sigma^2}{4G} + \frac{\Delta^2}{4H} - \frac{\lambda^3}{\pi^3} \sum_{i=-\infty}^{\infty} \sum_{k=-\infty}^{\infty} \sum_{l=-\infty}^{\infty} \Theta(\Lambda^2 - p_{ip}^2 - p_{kp}^2 - p_{lp}^2) \left[\mathcal{E}_{\Delta ikl}^{p+} + \mathcal{E}_{\Delta ikl}^{p-} \right], \quad (22)$$

where $\lambda = \pi/L$, $\mathcal{E}_{\Delta ikl}^{p\pm} = \sqrt{(\mathcal{E}_{ikl} \pm \mu)^2 + \Delta^2}$, $\mathcal{E}_{ikl} = \sqrt{p_{ip}^2 + p_{kp}^2 + p_{lp}^2 + \sigma^2}$, and $p_{ip} = 2i\lambda$ etc. In the periodic case it is very convenient to separate in each of the sums in (22) the contributions from zero modes, so the expression (22) can be rearranged in the following way:

$$\begin{aligned} \Omega_{Lp}(\sigma, \Delta) &= \frac{\sigma^2}{4G} + \frac{\Delta^2}{4H} - \frac{\lambda^3}{\pi^3} \left[\mathcal{E}_{\Delta 000}^{p+} + \mathcal{E}_{\Delta 000}^{p-} \right] - \frac{6\lambda^3}{\pi^3} \sum_{i=1}^{\infty} \Theta(\Lambda^2 - p_{ip}^2) \left[\mathcal{E}_{\Delta i00}^{p+} + \mathcal{E}_{\Delta i00}^{p-} \right] \\ &- \frac{12\lambda^3}{\pi^3} \sum_{i=1}^{\infty} \sum_{k=1}^{\infty} \Theta(\Lambda^2 - p_{ip}^2 - p_{kp}^2) \left[\mathcal{E}_{\Delta ik0}^{p+} + \mathcal{E}_{\Delta ik0}^{p-} \right] - \frac{8\lambda^3}{\pi^3} \sum_{i=1}^{\infty} \sum_{k=1}^{\infty} \sum_{l=1}^{\infty} \Theta(\Lambda^2 - p_{ip}^2 - p_{kp}^2 - p_{lp}^2) \left[\mathcal{E}_{\Delta ikl}^{p+} + \mathcal{E}_{\Delta ikl}^{p-} \right]. \end{aligned} \quad (23)$$

Now, as in the previous section, we interpret the quantities $\mathcal{E}_{\Delta ikl}^{p-}$ ($\mathcal{E}_{\Delta ikl}^{p+}$) in this expression as the energies of the fermion (antifermion) quasiparticles which can be labeled again by a triple of integers (i, k, l) with $i \geq k \geq l \geq 0$. Clearly, the quasiparticles of the type $(0, 0, 0)$ always contribute to the expression (23), whereas the contribution of the other energy levels depends on the λ -values. So, it is convenient, as in the case with antiperiodic boundary conditions, to divide the (μ, λ) plane into strips

$$\omega_1 = \{(\mu, \lambda) : \lambda > \lambda_1\}, \quad \omega_2 = \{(\mu, \lambda) : \lambda_1 > \lambda > \lambda_2\}, \quad \dots, \quad \omega_n = \{(\mu, \lambda) : \lambda_{n-1} > \lambda > \lambda_n\}, \quad \dots, \quad (24)$$

where for the real quantities λ_k we use the same notations as in Section III A, which now however take other values, i.e. $\lambda_1 = \sqrt{\Lambda^2/4} = 0.325$ GeV, $\lambda_2 = \sqrt{\Lambda^2/8} \approx 0.223$ GeV, $\lambda_3 = \sqrt{\Lambda^2/12} \approx 0.188$ GeV etc.⁵ The regions ω_n in (24) are constructed in such a way that in the strip ω_1 only the fermion and antifermion levels $(0, 0, 0)$ contribute to the TDP (23), where it looks like

$$\Omega_{Lp1}(\sigma, \Delta) = \frac{\sigma^2}{4G} + \frac{\Delta^2}{4H} - \frac{\lambda^3}{\pi^3} \left[\sqrt{(\sigma + \mu)^2 + \Delta^2} + \sqrt{(\sigma - \mu)^2 + \Delta^2} \right]. \quad (25)$$

⁵ As in the antiperiodic case, in the periodic one the real quantities $\lambda_{ikl} = \sqrt{\Lambda^2/N_{ikl}}$, where $N_{ikl} = 4(i^2 + k^2 + l^2)$, might be associated with corresponding energy level (i, k, l) . The real expressions $\lambda_1 > \lambda_2 > \lambda_3 > \dots$ in (24) are just the quantities λ_{ikl} arranged in a decreasing order.

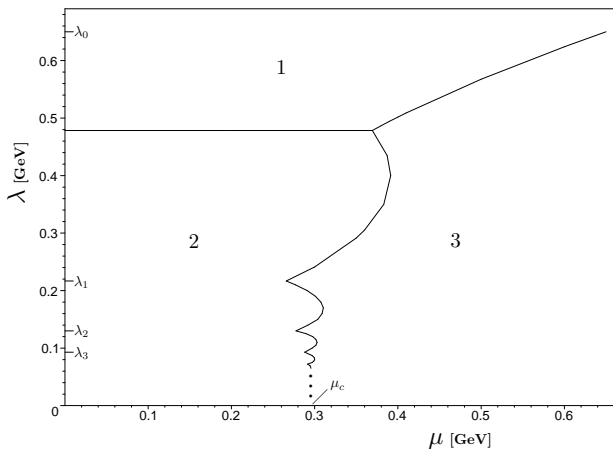


FIG. 9: Phase structure in the case of $R^2 \otimes S^1$ space topology with antiperiodic boundary conditions. Here $\lambda_k = \Lambda/(2k+1)$ ($k = 0, 1, 2, 3$) and other notations are given in Fig. 3.

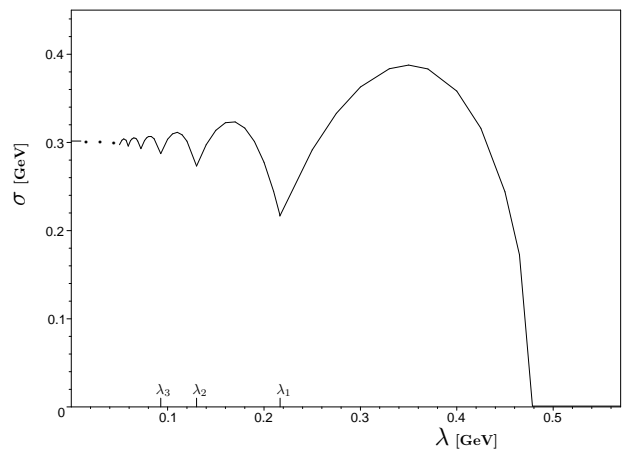


FIG. 10: The gap σ vs λ at $\mu = 0.2$ GeV in the case of $R^2 \otimes S^1$ space topology with antiperiodic boundary conditions. Here $\lambda_k = \Lambda/(2k+1)$ ($k = 1, 2, 3$).

(In this region there are no terms of the infinite sums of (23) which supply a nonzero contributions to the TDP.) In the strip ω_2 the energy levels $(1, 0, 0)$ of fermion and antifermion quasiparticles are switched on in addition, in the strip ω_3 the energy levels $(1, 1, 0)$ are switched on in addition, etc. Investigating the global minimum point behavior of the TDP (23) in each of the strips (24), it is possible to obtain the phase structure of the model in the whole (μ, λ) plane, which is presented in Fig. 8. The behavior of the gaps σ , Δ and particle density $n_\mu(\lambda)$ vs λ in the periodic case are qualitatively the same as in the case with antiperiodic boundary conditions (see Figs 4-7).

IV. THE CASE OF $R^2 \otimes S^1$ SPACE TOPOLOGY

In the present section we continue the investigation of the difermion condensation in the spaces with nontrivial topology, this time when it is of the form $R^2 \otimes S^1$. For simplicity, it is supposed here that the z -axis is compactified and fermion fields satisfy some boundary conditions of the form (the x, y coordinates are not restricted):

$$\psi_k(t, x, y, z + L) = e^{i\pi\alpha} \psi_k(t, x, y, z). \quad (26)$$

As in the previous section, we shall use only two values of the parameter α : $\alpha = 0$ for the periodic boundary condition and $\alpha = 1$ for the antiperiodic one. Recall that L is the length of the circumference S^1 . Note also that the consideration of any physical system in the above mentioned space topology is equivalent to a restriction of the system inside an infinite layer with thickness L . In this case, to obtain the thermodynamic potential $\Omega_{L\alpha}(M, \Delta)$ of the initial system, one again simply replaces the integration over p_3 in (14) by an infinite series, using the analogous rule:

$$\int_{-\infty}^{\infty} \frac{dp_3}{2\pi} f(p_3) \rightarrow \frac{1}{L} \sum_{n=-\infty}^{\infty} f(p_{n\alpha}), \quad p_{n\alpha} = \frac{\pi}{L}(2n + \alpha), \quad n = 0, \pm 1, \pm 2, \dots \quad (27)$$

A. The case of antiperiodic boundary conditions

Applying the rule (27) with $\alpha = 1$ in (14), one has for the TDP Ω_{La} of dense cold matter in a space of $R^2 \times S^1$ topology with antiperiodic boundary conditions the following expression

$$\Omega_{La}(\sigma, \Delta) = \frac{\sigma^2}{4G} + \frac{\Delta^2}{4H} - \frac{2\lambda}{\pi} \sum_{i=0}^{\infty} \int \frac{d^2p}{(2\pi)^2} \Theta(\Lambda^2 - \vec{p}^2 - p_{ia}^2) [\mathcal{E}_{\Delta i}^{a+} + \mathcal{E}_{\Delta i}^{a-}], \quad (28)$$

where $\lambda = \pi/L$, $\mathcal{E}_{\Delta i}^{a\pm} = \sqrt{(\mathcal{E}_i \pm \mu)^2 + \Delta^2}$, $\mathcal{E}_i = \sqrt{\vec{p}^2 + p_{ia}^2 + \sigma^2}$, and $p_{ia} = \lambda(2i+1)$. Recall that the quantities $\mathcal{E}_{\Delta i}^{a-}$ ($\mathcal{E}_{\Delta i}^{a+}$) are the energies of fermion (antifermion) quasiparticles, which are labeled by a discrete index i ($i = 0, 1, 2, \dots$) and by a continuous quantity $|\vec{p}|$. Integrating in (28) over two-dimensional momenta \vec{p} , we obtain

$$\Omega_{La}(\sigma, \Delta) = \frac{\sigma^2}{4G} + \frac{\Delta^2}{4H} + \frac{\lambda}{6\pi^2} \Theta\left(\frac{\Lambda - \lambda}{2\lambda}\right) \Phi_a(\sigma, \Delta), \quad (29)$$

where

$$\begin{aligned} \Phi_a(\sigma, \Delta) = & (N_a + 1) \left\{ 3\mu \left(\sqrt{\Lambda^2 + \sigma^2} + \mu \right) \sqrt{\left(\sqrt{\Lambda^2 + \sigma^2} + \mu \right)^2 + \Delta^2} - 2 \left[\left(\sqrt{\Lambda^2 + \sigma^2} + \mu \right)^2 + \Delta^2 \right]^{3/2} \right\} \\ & + \sum_{n=0}^{N_a} \left\{ 2 \left[\left(\sqrt{p_{na}^2 + \sigma^2} + \mu \right)^2 + \Delta^2 \right]^{3/2} - 3\mu \left(\sqrt{p_{na}^2 + \sigma^2} + \mu \right) \sqrt{\left(\sqrt{p_{na}^2 + \sigma^2} + \mu \right)^2 + \Delta^2} \right. \\ & \left. + 3\mu\Delta^2 \ln \left| \frac{\sqrt{\Lambda^2 + \sigma^2} + \mu + \sqrt{\left(\sqrt{\Lambda^2 + \sigma^2} + \mu \right)^2 + \Delta^2}}{\sqrt{p_{na}^2 + \sigma^2} + \mu + \sqrt{\left(\sqrt{p_{na}^2 + \sigma^2} + \mu \right)^2 + \Delta^2}} \right| \right\} + (\mu \rightarrow -\mu), \end{aligned} \quad (30)$$

and $N_a \equiv \left[\frac{\Lambda - \lambda}{2\lambda} \right]$ (recall, $[x]$ means the integer part of a real number x).

It is clear from the structure of the TDP (28)–(30) that to obtain the behavior of its global minimum point vs μ and λ it is very convenient to divide again the plane (μ, λ) into an infinite set of strips (20), this time with $\lambda_k = \Lambda/(2k+1)$.⁶ So, due to the presence of the Θ -function in (29), in the region ω_0 , i.e. at $\lambda > \lambda_0 \equiv \Lambda$, the TDP (28)–(29) has a trivial form, i.e.

$$\Omega_{La}(\sigma, \Delta) \Big|_{(\mu, \lambda) \in \omega_0} = \frac{\sigma^2}{4G} + \frac{\Delta^2}{4H}, \quad (31)$$

whose global minimum point ($\sigma = 0, \Delta = 0$) corresponds to the symmetric phase. In the region ω_1 , i.e. at $\lambda_0 > \lambda > \lambda_1$, the integer N_a from (30) is equal to zero, hence only quasiparticles with the energies $\mathcal{E}_{\Delta 0}^{a\pm}$ contribute to the TDP in this case. Studying the behavior of the GMP of the TDP vs μ and λ , we conclude that in the strip ω_1 three phases, the symmetric phase 1, the phase with broken chiral symmetry 2, and the superconducting phase 3, occur (see the part of Fig. 9 that corresponds to $\lambda_0 > \lambda > \lambda_1$). In the strip ω_2 we have in the expression (30) $N_a = 1$, so here the quasiparticle energies $\mathcal{E}_{\Delta 1}^{a\pm}$ contribute to the TDP in addition etc. However, our numerical calculations show that in each of the strips $\omega_2, \omega_3, \dots$ only two phases, the phase 2 and the SC phase 3, of the model are realized. The boundary between the phase with broken chiral symmetry 2 and the superconducting one 3 again oscillates when $\lambda \rightarrow 0$ (see Fig. 9). It turns out that in addition to the critical curve the gaps σ and Δ oscillate vs λ at fixed values of μ (see Figs 10, 11). Comparing these figures with Figs 4, 5, we see that the more dimensions are compactified, the more sharp oscillations of physical quantities occur. In particular, it is clear from Figs 10, 11 that in the case under consideration the gaps σ and Δ are some continuous functions vs λ , whereas in the case with $S^1 \otimes S^1 \otimes S^1$ space topology these quantities have discontinuities in the points λ_0, λ_1 , etc.

Finally, in Fig. 12 the ratio of particle densities $\frac{n_\mu(\lambda)}{n_\mu(0)}$ vs λ inside the SC phase is presented at $\mu = 0.4$ GeV. It is clear that in small vicinities around λ_k ($k = 2, 3, \dots$) the density at $\lambda \neq 0$ is less than the particle density at $\lambda = 0$. It seems intuitively clear that the smaller a particle density is, the easier a corresponding state of the system might be created. So to reduce the efforts in obtaining the SC phase, one could simply fix the λ -parameter not far from one of the λ_k -values. Hence finite size effects might promote the transition of a physical system into its superconducting phase.

B. The case of periodic boundary conditions

Clearly, to obtain the TDP of the system Ω_{Lp} in this case, it is necessary to use in (14) the rule (27) with $\alpha = 0$. As a result, we have

$$\begin{aligned} \Omega_{Lp}(\sigma, \Delta) = & \frac{\sigma^2}{4G} + \frac{\Delta^2}{4H} - \frac{\lambda}{\pi} \int \frac{d^2 p}{(2\pi)^2} \theta(\Lambda^2 - |\vec{p}|^2) \left[\mathcal{E}_{\Delta 0}^{p+} + \mathcal{E}_{\Delta 0}^{p-} \right] \\ & - \frac{2\lambda}{\pi} \sum_{n=1}^{\infty} \int \frac{d^2 p}{(2\pi)^2} \theta(\Lambda^2 - |\vec{p}|^2 - p_{np}^2) \left[\mathcal{E}_{\Delta n}^{p-} + \mathcal{E}_{\Delta n}^{p+} \right], \end{aligned} \quad (32)$$

where $\lambda = \pi/L$, $\mathcal{E}_{\Delta n}^{p\pm} = \sqrt{(\mathcal{E}_n \pm \mu)^2 + \Delta^2}$, $\mathcal{E}_n = \sqrt{\vec{p}^2 + p_{np}^2 + \sigma^2}$, $p_{np} = 2n\lambda$ ($n = 0, 1, 2, \dots$). Recall that the quantities $\mathcal{E}_{\Delta n}^{p-}$ ($\mathcal{E}_{\Delta n}^{p+}$) are the energies of fermion (antifermion) quasiparticles, which are labeled by a discrete index n

⁶ One should not become confused by the fact that we use the same notation for the boundaries λ_k of these strips in different cases. Indeed, as it is clear from the text, the value of each λ_k depends strongly on both the space topology and boundary conditions.

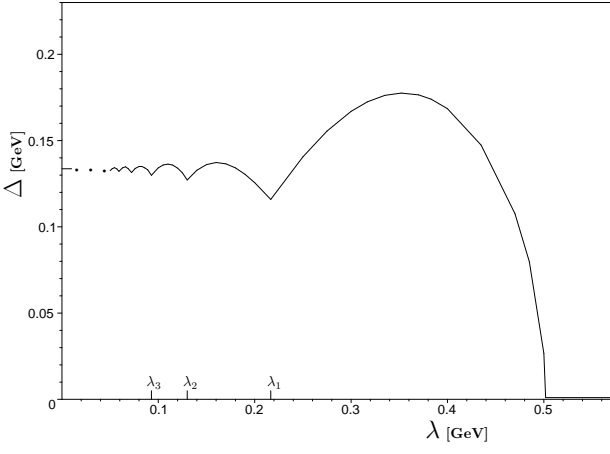


FIG. 11: The gap Δ vs λ at $\mu = 0.4$ GeV in the case of $R^2 \otimes S^1$ space topology with antiperiodic boundary conditions. Here $\lambda_k = \Lambda/(2k + 1)$ ($k = 1, 2, 3$).

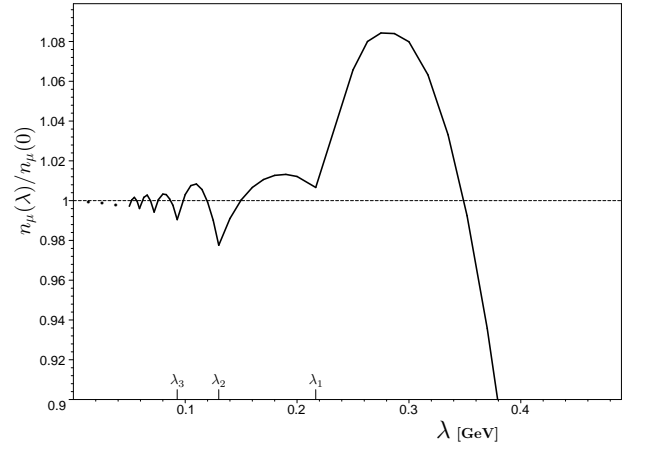


FIG. 12: Ratio of particle densities $\frac{n_\mu(\lambda)}{n_\mu(0)}$ vs λ at $\mu = 0.4$ GeV in the case of $R^2 \otimes S^1$ space topology with antiperiodic boundary conditions. Here $\lambda_k = \Lambda/(2k + 1)$ ($k = 1, 2, 3$).

($n = 0, 1, 2, \dots$) and by a continuous quantity $|\vec{p}|$, in addition. We find it convenient to separate in (32) the contribution from the zero modes, i.e. the contribution from quasiparticles with $n = 0$. Integrating in (32) over two-dimensional momenta \vec{p} , we have

$$\Omega_{Lp}(\sigma, \Delta) = \frac{\sigma^2}{4G} + \frac{\Delta^2}{4H} + \frac{\lambda}{12\pi^2} F(\sigma, \Delta) + \frac{\lambda}{6\pi^2} \Theta \left(\frac{\Lambda}{2\lambda} - 1 \right) \Phi_p(\sigma, \Delta), \quad (33)$$

where

$$\begin{aligned} F(\sigma, \Delta) &= 2 [(\sigma + \mu)^2 + \Delta^2]^{3/2} - 2 \left[(\sqrt{\Lambda^2 + \sigma^2} + \mu)^2 + \Delta^2 \right]^{3/2} \\ &+ 3\mu (\sqrt{\Lambda^2 + \sigma^2} + \mu) \sqrt{(\sqrt{\Lambda^2 + \sigma^2} + \mu)^2 + \Delta^2} - 3\mu(\sigma + \mu) \sqrt{(\sigma + \mu)^2 + \Delta^2} \\ &+ 3\mu\Delta^2 \ln \left| \frac{\sqrt{\Lambda^2 + \sigma^2} + \mu + \sqrt{(\sqrt{\Lambda^2 + \sigma^2} + \mu)^2 + \Delta^2}}{\sigma + \mu + \sqrt{(\sigma + \mu)^2 + \Delta^2}} \right| + (\mu \rightarrow -\mu), \end{aligned} \quad (34)$$

$$\begin{aligned} \Phi_p(\sigma, \Delta) &= N_p \left\{ 3\mu (\sqrt{\Lambda^2 + \sigma^2} + \mu) \sqrt{(\sqrt{\Lambda^2 + \sigma^2} + \mu)^2 + \Delta^2} - 2 \left[(\sqrt{\Lambda^2 + \sigma^2} + \mu)^2 + \Delta^2 \right]^{3/2} \right\} \\ &+ \sum_{n=1}^{N_p} \left\{ 2 \left[(\sqrt{p_{np}^2 + \sigma^2} + \mu)^2 + \Delta^2 \right]^{3/2} - 3\mu (\sqrt{p_{np}^2 + \sigma^2} + \mu) \sqrt{(\sqrt{p_{np}^2 + \sigma^2} + \mu)^2 + \Delta^2} \right. \\ &\left. + 3\mu\Delta^2 \ln \left| \frac{\sqrt{\Lambda^2 + \sigma^2} + \mu + \sqrt{(\sqrt{\Lambda^2 + \sigma^2} + \mu)^2 + \Delta^2}}{\sqrt{p_{np}^2 + \sigma^2} + \mu + \sqrt{(\sqrt{p_{np}^2 + \sigma^2} + \mu)^2 + \Delta^2}} \right| \right\} + (\mu \rightarrow -\mu), \end{aligned} \quad (35)$$

and $N_p \equiv \lceil \frac{\Lambda}{2\lambda} \rceil$ is the integer part of the real number in the square bracket.

As in section III B, we again divide the (μ, λ) -plane into an infinite set of strips ω_k (24), where in the present case we have $\lambda_k = \Lambda/(2k)$ ($k = 1, 2, \dots$). Then, in the region ω_1 the zero energy levels $\mathcal{E}_{\Delta 0}^{p\pm}$ of quasiparticles contribute to the TDP (32), where it looks like

$$\Omega_{Lp}(\sigma, \Delta) \Big|_{(\mu, \lambda) \in \omega_1} = \frac{\sigma^2}{4G} + \frac{\Delta^2}{4H} + \frac{\lambda}{12\pi^2} F(\sigma, \Delta) \quad (36)$$

(here $F(\sigma, \Delta)$ is given in (34)). In the region ω_2 the next energy levels $\mathcal{E}_{\Delta 1}^{p\pm}$ are switched on in addition, so in the expression for the function $\Phi_p(\sigma, \Delta)$ (35) we have $N_p = 1$, etc. It turns out that with each region ω_k ($k \geq 2$) the value $N_p = k - 1$ in (35) is associated. As a result, in ω_k all the quasiparticle energy levels with quantum numbers

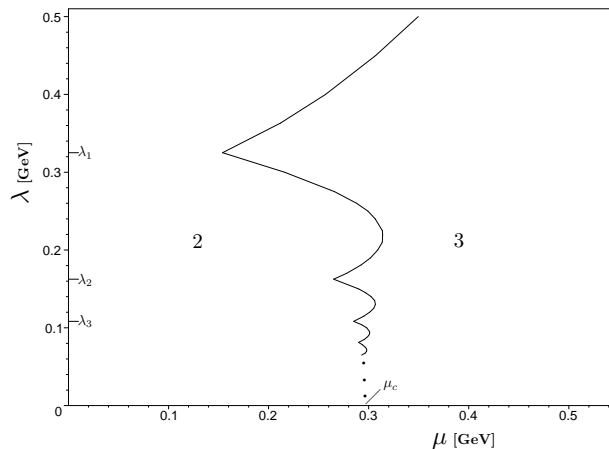


FIG. 13: Phase structure in the case of $R^2 \otimes S^1$ space topology with periodic boundary conditions. Here $\lambda_k = \Lambda/(2k)$ ($k = 1, 2, 3$), and the numbers 2,3 denote the chirally broken and SC phases.

$n = 0, 1, \dots, k - 1$ contribute to the expression for the TDP. Studying numerically step-by-step the behavior of the GMP of the TDP (33) in the strips $\omega_0, \omega_1, \omega_2, \dots$, we obtain the (μ, λ) phase portrait of the initial NJL model which is presented in Fig. 13. In contrast to the phase portrait in the antiperiodic case (see Fig. 9), it has only two phases, the chirally broken phase 2 and the superconducting one 3.

Notice that in the case with periodic boundary conditions the behavior of the gaps σ , Δ and particle density $n_\mu(\lambda)$ are qualitatively the same as in the antiperiodic case (see Figs 10 – 12).

V. SUMMARY AND DISCUSSION

In the present paper we have investigated the influence of finite-size effects on the superconductivity (SC) phenomenon which might exist in dense cold fermionic matter. Note that in the SC phase the $U(1)$ charge group is spontaneously broken down due to Cooper pair (difermion) condensation. It is well-known that quantum fluctuations of fields can destroy symmetry breaking in a finite volume, so studying this effect requires to be sure that such fluctuations and their corresponding next to leading order corrections will not spoil the leading order mean field results. Concerning the application of usual QCD-like NJL models to the description of CSC in the mean field approximation, a small perturbative expansion parameter guaranteeing the suppression of quantum fluctuations is absent. Thus, in this case there is no confidence that quantum fluctuations are in general negligible and, particularly in the case of finite systems, that they could not destroy color symmetry breaking. These obstacles were the main reason why we decided to consider instead of a QCD-like quark model the “toy” NJL model (1) for fermions which seems to us technically more adequate for studying the influence of finite volume effects on the Cooper pairing. In fact, in this model at large N a small expansion parameter $1/N$ appears, so the next to leading order corrections in $1/N$ are certainly negligible. By this reason, quantum fluctuations of fields become suppressed and cannot destroy spontaneous symmetry breaking for the considered fermion system in a finite volume (see also the discussion in Introduction).

Let us summarize in more detail some of the main results. First, it was shown in the leading order of the $1/N$ -expansion that at $T = 0, L = \infty$ (L is the linear size of the system) there is a phase transition in the considered fermion model from the chiral symmetry breaking phase 2 to a superconducting one 3 at the critical value of the chemical potential $\mu = \mu_c \approx 0.3$ GeV. Next, we have studied in the leading order over $1/N$ the phase structure of this model both in the space with topology $S^1 \otimes S^1 \otimes S^1$ and $R^2 \otimes S^1$ taking into account periodic and antiperiodic boundary conditions for fermion fields. It turns out that for all cases the critical line between phase 2 and 3 as well as the gaps σ , Δ and the particle density $n_\mu(\lambda)$ are oscillating functions vs $\lambda \sim 1/L$. Generally we found that the more spatial dimensions are compactified, the stronger oscillations occur.

Secondly, it is interesting to note that at finite L the superconducting phase 3 might be realized at sufficiently smaller values of the chemical potential μ and particle density $n_\mu(\lambda)$, than at $L = \infty$. Indeed, as it is clear from, e.g., Figs. 3, 13 for some values of λ the phase 3 occurs at $\mu = 0.2$ GeV or even smaller values. Moreover, as it is clear from the discussion at the end of section III A, for such sufficiently small values of μ the particle density inside the SC phase might be as small as $\approx 0.4 n_c$, where n_c is the density at which SC is realized at $L = \infty$. Hence, the compactification procedure itself might shift the SC phase transition to smaller particle densities.

Hopefully, the above investigations could motivate other studies of finite size effects and eventually find some physical applications.

Acknowledgments

One of us (K.G.K.) is grateful to Prof. M. Mueller-Preussker and his colleagues for the kind hospitality at the Institute of Physics of the Humboldt-University during November – December of 2009 and to *Deutscher Akademischer Austauschdienst* (DAAD) for financial support.

-
- [1] Y. Nambu and G. Jona-Lasinio, Phys. Rev. **124**, 246 (1961).
 [2] D. Ebert, Yu. L. Kalinovsky, L. Münchow and M. K. Volkov, Int. J. Mod. Phys.A **8**, 1295 (1993).
 [3] D. Ebert, H. Reinhardt and M. K. Volkov, Prog. Part. Nucl. Phys. **33**,1 (1994); S. P. Klevansky, Rev. Mod. Phys. **64**, 649 (1992); T. Hatsuda and T. Kunihiro, Phys. Rept. **247**, 221 (1994).
 [4] M. Asakawa and K. Yazaki, Nucl. Phys. A **504**, 668 (1989); P. Zhuang, J. Hüfner and S. P. Klevansky, Nucl. Phys. A **576**, 525 (1994).
 [5] B. Hiller, A. A. Osipov, A. H. Blin and J. da Providencia, Phys. Lett. B **650**, 262 (2007); E. S. Fraga and A. J. Mizher, Phys. Rev. D **78**, 025016 (2008); Nucl. Phys. A **831**, 91 (2009); H. Abuki, R. Anglani, R. Gatto, G. Nardulli and M. Ruggieri, Phys. Rev. D **78**, 034034 (2008); A. Ayala, A. Bashir, A. Raya and A. Sanchez, Phys. Rev. D **80**, 036005 (2009); AIP Conf. Proc. **1116** (2009) 128; A. J. Mizher, M. N. Chernodub and E. S. Fraga, arXiv:1004.2712.
 [6] H. J. Warringa, D. Boer and J. O. Andersen, Phys. Rev. D **72**, 014015 (2005); D. Boer and J. K. Boomsma, Phys. Rev. D **78**, 054027 (2008); Phys. Rev. D **80**, 034019 (2009).
 [7] M. Buballa, Phys. Rept. **407**, 205 (2005); M. Huang, Int. J. Mod. Phys. E. **14**, 675 (2005); I. A. Shovkovy, Found. Phys. **35**, 1309 (2005); K. G. Klimenko and D. Ebert, Theor. Math. Phys. **150**, 82 (2007); M. G. Alford, A. Schmitt, K. Rajagopal, and T. Schäfer, Rev. Mod. Phys. **80**, 1455 (2008).
 [8] D. Ebert and M. K. Volkov, Yad. Fiz. **36**, 1265 (1982); D. Ebert and H. Reinhardt, Nucl. Phys. B **271**, 188 (1986).
 [9] D. Ebert and K. G. Klimenko, Nucl. Phys. A **728**, 203 (2003); T. Inagaki, D. Kimura, and T. Murata, Prog. Theor. Phys. Suppl. **153**, 321 (2004); L. Campanelli and M. Ruggieri, Phys. Rev. D **80**, 034014 (2009); D. P. Menezes, M. B. Pinto, S. S. Avancini, A. P. Martinez and C. Providencia, Phys. Rev. C **79**, 035807 (2009); D. P. Menezes, M. B. Pinto, S. S. Avancini and C. Providencia, Phys. Rev. C **80**, 065805 (2009); J. K. Boomsma and D. Boer, arXiv:0911.2164.
 [10] K. G. Klimenko, Theor. Math. Phys. **90**, 1 (1992); Z. Phys. C **54**, 323 (1992); V. P. Gusynin, V. A. Miransky, and I. A. Shovkovy, Phys. Lett. B **349**, 477 (1995); M. A. Vdovichenko, A. S. Vshivtsev and K. G. Klimenko, Phys. Atom. Nucl. **63**, 470 (2000).
 [11] K. G. Klimenko, B. V. Magnitsky and A. S. Vshivtsev, Phys. Atom. Nucl. **57**, 2171 (1994); Nuovo Cim. A **107**, 439 (1994); I. A. Shovkovy and V. M. Turkowski, Phys. Lett. B **367**, 213 (1996); D. Ebert and V.C. Zhukovsky, Mod. Phys. Lett. A **12**, 2567 (1997).
 [12] T. Inagaki, T. Muta and S. D. Odintsov, Prog. Theor. Phys. Suppl. **127**, 93 (1997).
 [13] E. Elizalde, S. Leseduarte and S. D. Odintsov, Phys. Rev. D **49**, 5551 (1994); E. Elizalde, S. D. Odintsov and Yu. I. Shilnov, Mod. Phys. Lett. A **9**, 913 (1994); G. Miele and P. Vitale, Nucl. Phys. B **494**, 365 (1997); D. K. Kim and K. G. Klimenko, J. Phys. A **31**, 5565 (1998).
 [14] S. K. Kim, W. Namgung, K. S. Soh, and J. H. Yee, Phys. Rev. D **36**, 3172 (1987); D. Y. Song and J. K. Kim, Phys. Rev. D **41**, 3165 (1990); A. S. Vshivtsev, K. G. Klimenko, B. V. Magnitsky, JETP Lett. **61**, 871 (1995); Phys. Atom. Nucl. **59**, 529 (1996); A. S. Vshivtsev, A. G. Kisun'ko, K. G. Klimenko, and D. V. Peregudov, Izv. Vuz. Fiz. **41N2**, 29 (1998); M. A. Vdovichenko and A. K. Klimenko, JETP Lett. **68**, 460 (1998); V. Schon and M. Thies, arXiv:hep-th/0008175.
 [15] I. V. Krive and S. A. Naftulin, Nucl. Phys. B **364**, 541 (1991); D. K. Kim, Y. D. Han and I. G. Koh, Phys. Rev. D **49**, 6943 (1994); A. V. Gamayun and E. V. Gorbar, Phys. Lett. B **610**, 74 (2005).
 [16] D. K. Kim and I. G. Koh, Phys. Rev. D **51**, 4573 (1995); A. S. Vshivtsev, M. A. Vdovichenko and K. G. Klimenko, J. Exp. Theor. Phys. **87**, 229 (1998); E. J. Ferrer, V. P. Gusynin and V. de la Incera, Phys. Lett. B **455**, 217 (1999); E. J. Ferrer and V. de la Incera, TSPU Vestnik **44N7**, 88 (2004); L. M. Abreu, A. P. C. Malbouisson, J. M. C. Malbouisson and A. E. Santana, Nucl. Phys. B **819**, 127 (2009); M. Hayashi and T. Inagaki, arXiv:1003.1173; arXiv:1003.3163.
 [17] J. Madsen, Lect. Notes Phys. **516**, 162 (1999) [arXiv:astro-ph/9809032].
 [18] L. F. Palhares, E. S. Fraga and T. Kodama, arXiv:0904.4830; PoS **CPOD2009**, 011 (2009) [arXiv:0910.4363].
 [19] D. Ebert, K. G. Klimenko and H. Toki, Phys. Rev. D **64**, 014038 (2001); V. C. Zhukovsky, V. V. Khudiyakov, K. G. Klimenko and D. Ebert, JETP Lett. **74**, 523 (2001); Phys. Rev. D **65**, 054024 (2002).
 [20] E. J. Ferrer and V. de la Incera, Phys. Rev. D **76**, 045011 (2007); E. J. Ferrer, V. de la Incera and C. Manuel, Nucl. Phys. B **747**, 88 (2006).
 [21] D. Ebert, A. V. Tyukov and V. C. Zhukovsky, Phys. Rev. D **76**, 064029 (2007); Phys. Rev. D **80**, 085019 (2009).
 [22] J. Madsen, Phys. Rev. Lett. **87**, 172003 (2001); J. Phys. G **28**, 1737 (2002); O. Kiriyama, Int. J. Mod. Phys. A **21**, 3021 (2006).
 [23] N. D. Mermin and H. Wagner, Phys. Rev. Lett. **17**, 1133 (1966); S. Coleman, Commun. Math. Phys. **31**, 259 (1973).
 [24] A.V. Veryaskin, V.G. Lapchinskii, and V.A. Rubakov, Teor. Mat. Fiz. **45**, 407 (1980); G. Denardo and E. Spalucci, Class. Quantum Grav. **6**, 1915 (1989); D. Ebert, K. G. Klimenko, A. V. Tyukov and V. C. Zhukovsky, Eur. Phys. J. C **58**, 57 (2008).
 [25] A. Barducci, R. Casalbuoni, M. Modugno and G. Pettini, Phys. Rev. D **51**, 3042 (1995).
 [26] D. Ebert, K. G. Klimenko, A. V. Tyukov and V. C. Zhukovsky, Phys. Rev. D **78**, 045008 (2008).